Rhodium-Catalyzed [5 + 1 + 2] Cycloaddition of Yne-3-Acyloxy-1,4-Enynes (YACEs) and Carbon Monoxide: Reaction Development and Mechanism

Qi Cui,† Pan Zhang,† Bing-Wen Li,† Yi Jin, Qianwei Zhang, Hong-Xi Bai, and Zhi-Xiang Yu*
Beijing National Laboratory for Molecular Sciences (BNLMS), Key Laboratory of Bioorganic Chemistry and Molecular Engineering of Ministry of Education, College of Chemistry, Peking University, Beijing 100871, China.

ABSTRACT: Developing new reaction to synthesize challenging eight-membered carbocycles is a research frontier of organic synthesis. Reported here is the development of the first Rh-catalyzed [5 + 1 + 2] cycloaddition of yne-3-acyloxy-1,4-enyne (Yne-ACEs, short as YACEs) and CO, in which sequentially 5-carbon (generated from 3-acyloxy-1,4-enynes), 1-carbon (CO) and 2-carbon (alkynes) are embedded into the final 5/8 scaffold containing cyclooctatrienone structure. This reaction has broad scope and can be carried out under mild conditions. Keys to the success of the present [5 + 1 + 2] reaction, discovered and supported by experiments and *ab initio* calculations, include: using terminal alkyne in the 3-acyloxy-1,4-enyne moiety of the substrates so that 1,2-acyloxy migration (instead of 1,3-acyloxy migration, a step required for competing [4 + 2 + 1] reaction) can be realized; applying electron-rich aryl group (here is *p*-dimethylamino aryl) in the acyloxy group to make [5 + 1] pathway disfavored. Quantum chemical calculations have also been used to answer why this reaction is [5 + 1 + 2] but not [5 + 2 + 1] (where alkyne insertion is ahead of CO insertion), and the factors disfavoring the competitive [5 + 2], [5 + 1] and [4 + 2 + 1] reactions.

INTRODUCTION

Seven- and eight-membered carbocycles are widely found in natural products and bioactive molecules. However, synthesis of these molecules is still posing challenges because available methods and strategies for accessing these medium-sized rings are limited.[1] Due to this, there are tremendous and unceasing efforts from the synthetic organic chemistry community to develop new reactions, especially transition-metal catalyzed cycloadditions, to access seven- and eight-membered carbocycles.[2] Two transition metal catalyzed reactions for the synthesis of seven-membered carbocycles are given in Scheme 1. The first one is Tang's [5 + 2] reaction[3] of yne-3-acyloxy-1,4-enynes (yne-ACEs, also short as YACEs) (Scheme 1A) and the other is our [4 + 2 + 1] reaction of *in situ* generated ene/yne-ene-allenes and CO (Scheme 1B).[4] Tang's [5 + 2] reaction starts from 1,2-acyloxy migration, followed by alkyne insertion and reductive elimination, which has been supported by DFT calculations (the 2π component can also be alkenes and this is not shown in Scheme 1A).[5] In our [4 + 2 + 1] reaction, a pathway involving 1,3-acyloxy migration, oxidative cyclization, CO insertion and reductive elimination has been proposed and supported computationally.[5,6]

With the previous success of [4 + 2 + 1] reaction of the *in situ* generated ene/yne-ene-allenes and CO, we then hypothesized whether YACEs could also undergo [4 + 2 + 1] reaction when CO is present, wishing to construct highly functionalized seven-membered carbocycles (Scheme 1C, see also the proposed pathway in Figure 1 and initial experimental tests shown in Figure 2). To realize this, the desired reaction has to start from a 1,3-acyloxy migration, instead of a 1,2-acyloxy migration which is required for Tang's [5 + 2] reaction (see Figure 1 for the proposed mechanism). Therefore, choosing an appropriate R^1 group in the substrates was critical to tune the selectivity for different cycloadditions. Actually, we tested this idea, finding that, when R^1 = electron-donating group such as methyl, phenyl and 4-(benzyloxy)phenyl, the [4 + 2 + 1] reactions were achieved (Figure 2A, details are given in the Supporting Information (SI)). We were happy to find this new [4 + 2 + 1] reaction. But when R^1 = electron-withdrawing group such as ethoxycarbonyl and trifluoromethyl, 1,2-acyloxy migration was favored, and in this case, only Tang's [5 + 2] reaction happened, without forming CO-inserted product (Figure 2B). To our surprise, when R^1

= H, we got neither [5 + 2] products nor [4 + 2 + 1] products, but [5 + 1 + 2] products (see later on discussion of naming this reaction) and [5 + 1][3g,7] products (Figure 2C).

Scheme 1. Tang's [5 + 2] Cycloaddition, Our Previous [4 + 2 + 1] Cycloaddition and This Work

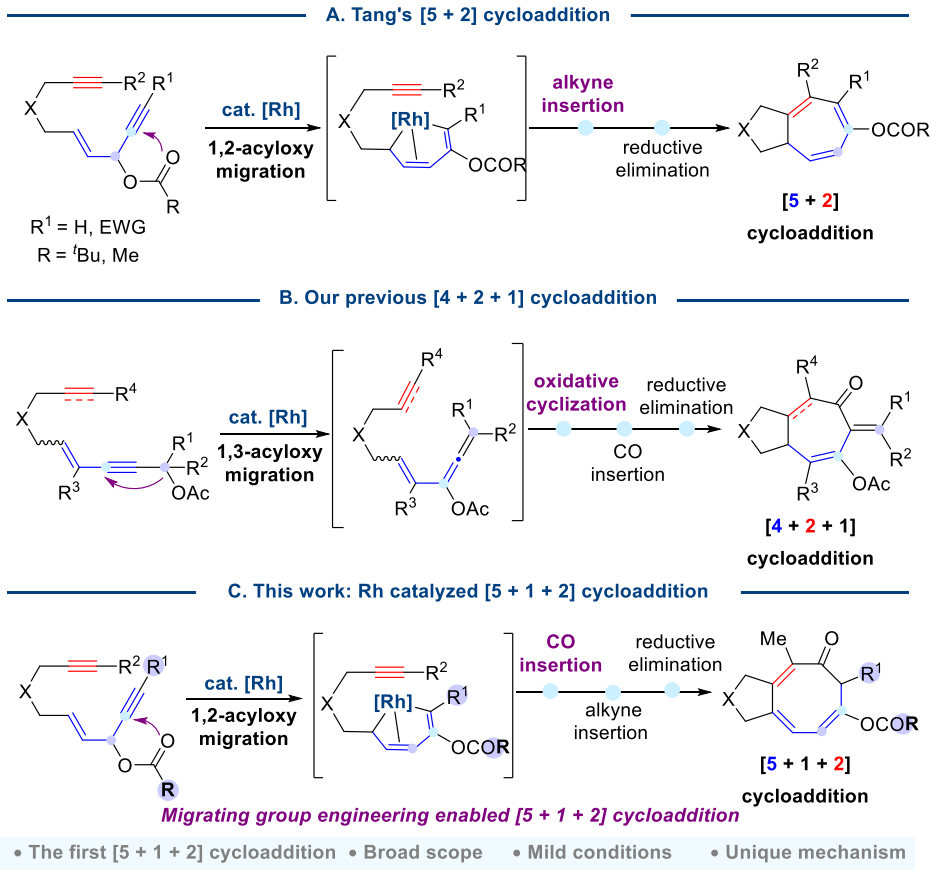

The proposed mechanism for the new [5 + 1 + 2] reaction of YACEs and CO, supported by subsequent quantum chemical calculations (also detailed in this paper), is illustrated in Figure 1. In this cycloaddition, key intermediate **V** favors CO and alkyne insertions, followed by reductive elimination and a [1,5]-H shift. We named this reaction as [5 + 1 + 2] because CO insertion occurs before the alkyne insertion. If alkyne insertion first and then CO insertion take place, the reaction can be named as [5 + 2 + 1] reaction, which is disfavored compared to the [5 + 1 + 2] reaction (see discussion in the results and discussion section). The [5 + 1] reaction pathway is also depicted in Figure 1 and had been investigated (this will be discussed in the mechanistic section of this paper). Intrigued by this serendipitous discovery and prompted by the high demand of reactions synthesizing eight-membered carbocycles, we decided to develop this [5 + 1 + 2] reaction[8] as a general method to reach highly functionalized eight-membered ring compounds, which is present in this paper (Scheme 1C). Of the same importance, mechanism of this reaction, effects of substituents and migrating groups are also present here to understand why we can succeed, which will be helpful for understanding the present reaction and other cycloadditions catalyzed by transition metals.

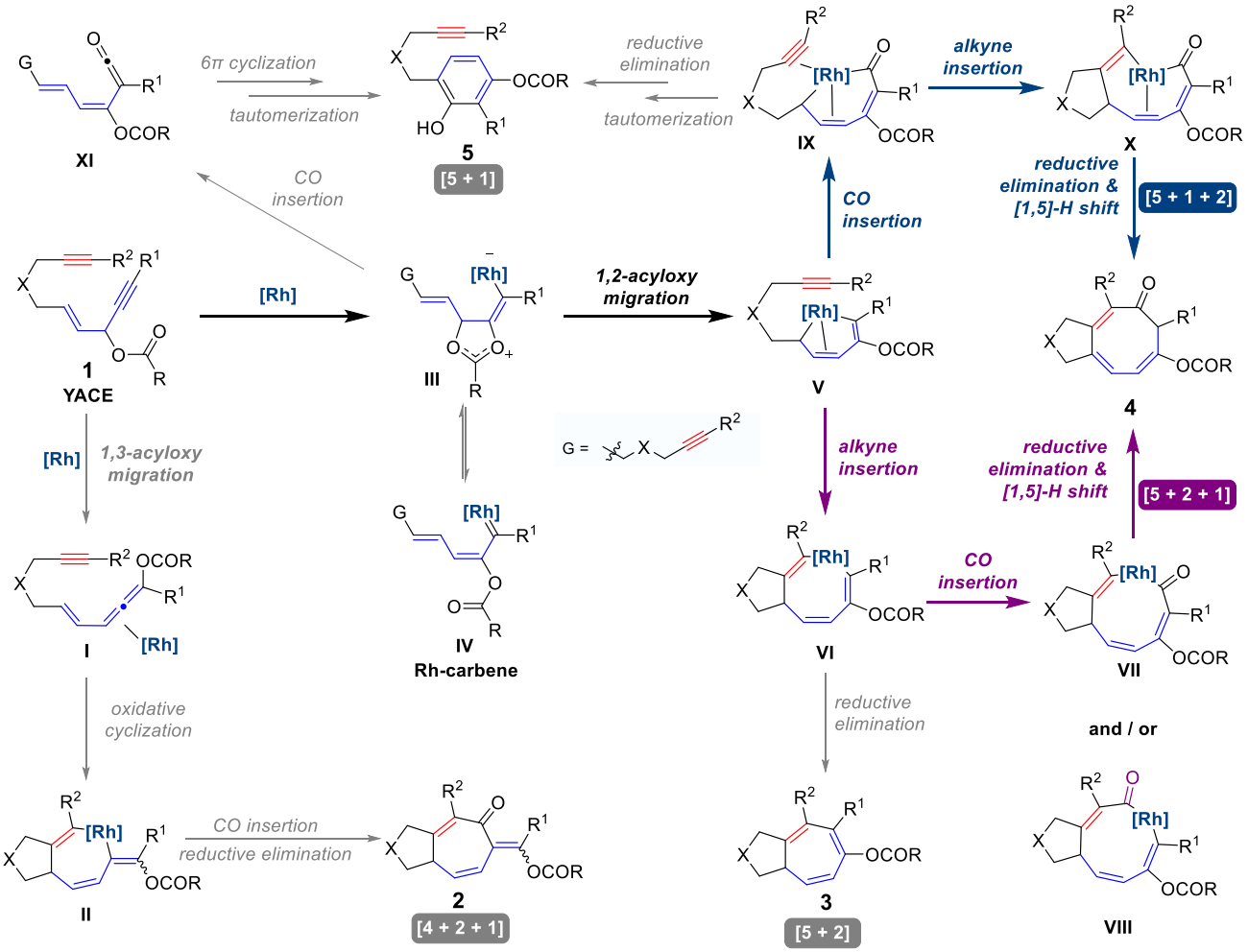

Figure 1. Proposed pathways for [4 + 2 + 1], [5 + 2 + 1] or [5 + 1 + 2], [5 + 2], and [5 + 1] cycloadditions of YACEs and CO catalyzed by Rh.

RESULTS AND DISCUSSION

Reaction Optimization of [5 + 1 + 2] Reaction of YACEs and CO

We screened reaction conditions (solvent, temperature, CO pressure et al.) for this new [5 + 1 + 2] cycloaddition using **1f** as a model substrate, finding that the highest yield of the 5/8 product **4f** was only 29% (see SI for more details). The yield of [5 + 1 + 2] cycloadduct (no other side product was isolated) was 33% when 120 mol % $[Rh(CO)_2Cl]_2$ was used. Using either $Co_2(CO)_8$ or $Ir(CO)(PPh_3)_2Cl$ as the catalyst did not accomplish the target [5 + 1 + 2] reaction. We speculated the [5 + 1 + 2] product with a triene unit could act as a ligand coordinating to the Rh catalyst and consequently deactivating the catalytic species. This hypothesis can be ruled out, because carrying out the [5 + 1 + 2] reaction of **1f** in the presence of **4f** did not experience a decreased reaction yield (it was about 30%).

We then turned our attention to modulate the R group in YACEs that could accelerate and favor the 1,2-acyloxy migration required for the [5 + 1 + 2] reaction. Otherwise, the substrate could have some side reactions (such as alkyne cyclotrimerization to form benzene derivatives, also catalyzed by Rh). We envisioned that an electron-rich R group in the acyloxy group of the YACEs was a good choice to realize the above design (Figure 2D). Actually, Tang and coworkers once investigated the migrating ability of several acyloxy groups in their study of [5 + 2] cycloaddition reactions, discovering that 4-methyloxybenzolate (R=4-C_6H_4OMe ester) and *N,N*-dimethyl-4-aminobenzoate (R=4-$C_6H_4NMe_2$) can greatly accelerate the 1,2-migration process and promote their [5 + 2] cycloadditions. We experimentally tested substrate **1h** with R= 4-C_6H_4OMe, finding that the reaction yield of [5 + 1 + 2] can be improved

to 41% (see SI). This encouraged us to screen more electron-rich acyloxy groups. To our delight, substrate **1i** with R=4-$C_6H_4NMe_2$ gave improved reaction yields, which then encouraged us to optimize the reaction conditions by using this substrate (Table 1).

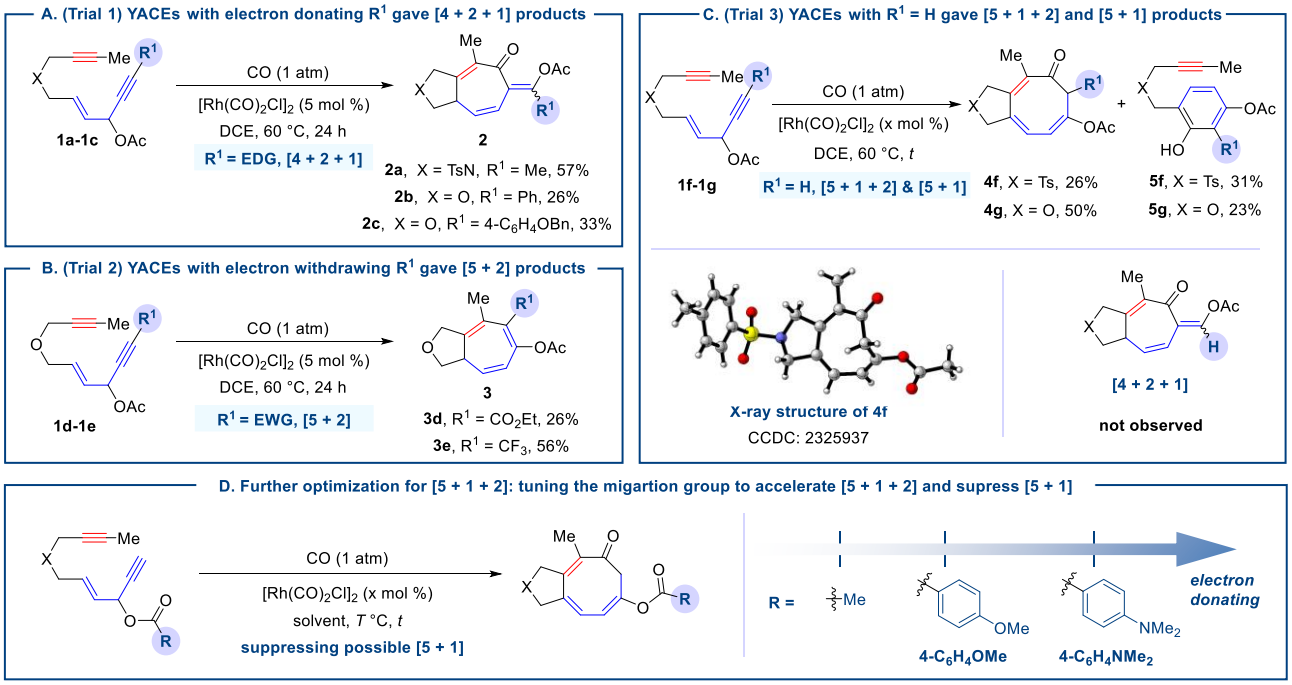

Figure 2. Initial study of [5 + 1 + 2] cycloaddition. EDG, electron donating group; EWG, electron withdrawing group. Reaction conditions: **1** (0.1 mmol), $[Rh(CO)_2Cl]_2$ (5 mol %), DCE (4 mL), 60 °C, CO (1 atm). The yield for each substrate reported was an average of two runs unless otherwise specified. For substrate **1f**, x = 10, t = 14 h; for substrate **1g**, x = 5, t = 24 h.

Solvent screening indicated that dioxane gave the highest reaction yield than others we tested: 18% (DCE), 26% (THF), 38% (toluene), 53% (acetonitrile), 68% (dioxane) (Table 1, entries 1-5). Using 0.2 atmosphere of CO was not beneficial to the [5 + 1 + 2] reaction, with a reaction yield of 56% (Table 1, entry 6). Decreasing the concentration of **1i** to 0.01 M did not improve the reaction outcome, where **4i** was obtained in 67% yield (Table 1, entry 7). The yields of the [5 + 1 + 2] reactions were 57% and 67% respectively when raising or lowering the reaction temperature (60 °C or 30 °C) (Table 1, entries 8-9). We hypothesized that, the cyclooctatrienone product may coordinate with rhodium catalyst and interference the isolation of the final product. Therefore, we added 1.2 equivalent of PPh_3 to the reaction mixture once the reaction was finished. To our disappointment, we did not get an improved reaction yield in this case (Table 1, entry 10). Further study showed that cationic catalyst of $Rh(COD)_2SbF_6$ can also catalyze this [5 + 1 + 2] cycloaddition, but the reaction was not clean and the reaction yield was only 29% (Table 1, entry 11). Based on these results in Table 1, we chose the reaction conditions in entry 5 of Table 1 as the optimal ones for further study of reaction scope.

Table 1. Reaction Optimization of [5 + 1 + 2] Cycloaddition Using Substrate 1i and CO

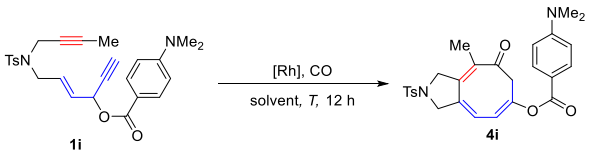

Entry[a]	Catalyst		$P_{(CO)}$	Solvent	Conc.	T	Yield[b]
1	$[Rh(CO)_2Cl]_2$	5 mol %	1 atm	DCE	0.025 M	40 °C	18%
2	$[Rh(CO)_2Cl]_2$	5 mol %	1 atm	THF	0.025 M	40 °C	26%
3	$[Rh(CO)_2Cl]_2$	5 mol %	1 atm	Toluene	0.025 M	40 °C	38%
4	$[Rh(CO)_2Cl]_2$	5 mol %	1 atm	MeCN	0.025 M	40 °C	53%[c]
5	**$[Rh(CO)_2Cl]_2$**	**5 mol %**	**1 atm**	**Dioxane**	**0.025 M**	**40 °C**	**68%**
6	$[Rh(CO)_2Cl]_2$	5 mol %	0.2 atm	Dioxane	0.025 M	40 °C	56%
7	$[Rh(CO)_2Cl]_2$	5 mol %	1 atm	Dioxane	0.01 M	40 °C	67%
8	$[Rh(CO)_2Cl]_2$	5 mol %	1 atm	Dioxane	0.025 M	60 °C	57%
9	$[Rh(CO)_2Cl]_2$	5 mol %	1 atm	Dioxane	0.025 M	30 °C	67%
10	$[Rh(CO)_2Cl]_2$	5 mol %	1 atm	Dioxane	0.025 M	40 °C	62%[d]
11	$Rh(COD)_2SbF_6$	10 mol %	1 atm	Dioxane	0.025 M	40 °C	29%

[a] All the reactions were performed on 0.05 mmol scale, [b] ^{1}H-NMR yield using dibromomethane as an internal standard. [c] The conversion was 71% based on ^{1}H-NMR spectrum. [d] After 12 h, PPh_3 (1.2 eq.) was added and the reaction was stirred for 2 h.

Reaction Scope of [5 + 1 + 2] Reaction

Here we performed the [5 + 1 + 2] reactions for all tested substrates in a 0.1 mmol scale (Figure 3). Substrates with R^1= alkyl group such as methyl, ethyl, and butyl groups gave [5 + 1 + 2] products with reaction yields of 60%, 65%, and 68%, respectively. Notably, [5 + 1 + 2] cycloaddition of **1l** with a vinyl substitution had a poor conversion within 12 hours. Fortunately, the reaction yield can reach 34% with an extended reaction time of 36 hours. For substrates **1m** and **1n** with aryl groups, the corresponding [5 + 1 + 2] cycloadditions occurred smoothly, with reaction yields of 63% and 74%, respectively. The present [5 + 1 + 2] cycloaddition was suitable for substrates with a diester tether, as demonstrated by the reaction of **1o** to **4o** in 52% yield.

To our delight, substrates with oxygen tether were suitable for the [5 + 1 + 2] reaction (see substrates **1p**-**1t** in Figure 3). Importantly, their corresponding [5 + 1 + 2] cycloadducts had good solubility and can be easily purified by flash column chromatography. Substrate **1p** with R^3=Ph gave **4p** in a 58% yield. One special case in the present [5 + 1 + 2] reaction was found for substrate **1q** with a terminal alkyne as its 2π component, which gave both the initially formed [5 + 1 + 2] product **4q'** and the final product **4q,** generated from **4q'** via [1,5]-H shift (the ratio of **4q** and **4q'** was 1:5). The reaction yields for *O*-tethered substrates with R^2=Me, 4-C_6H_4Br and 4-$C_6H_4CO_2$Me were 67%, 69%, and 52%, respectively. **We also tested substrate with an alkene as the 2π component, finding that ene-ACE substrate failed to deliver the [5 + 1 + 2] cycloadduct** (see the SI for details). It is worthwhile to note that neither [4 + 2 + 1] nor [5 + 1] cycloadduct was detected for all substrates shown in Figure 3.

We explored whether the three-component [5 + 1 + 2] cycloaddition by using *n*-Pr substituted 3-acyloxy-1,4-enyne, 3-hexyne (**1u**) and CO under the standard conditions can occur (Scheme 2). No desired intermolecular product was detected, but only 13% of [5 + 1] cycloaddition product **5u** was isolated.

Scheme 2. Attempt to Achieve Three-Component [5 + 1 + 2] Reaction of ACE, CO, and Alkyne

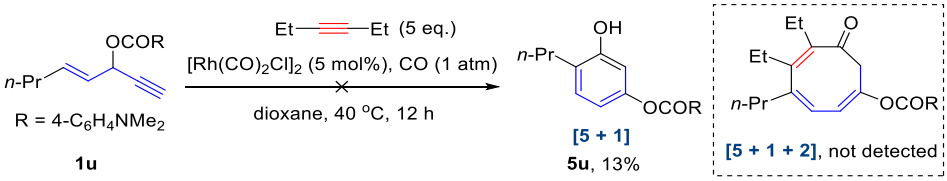

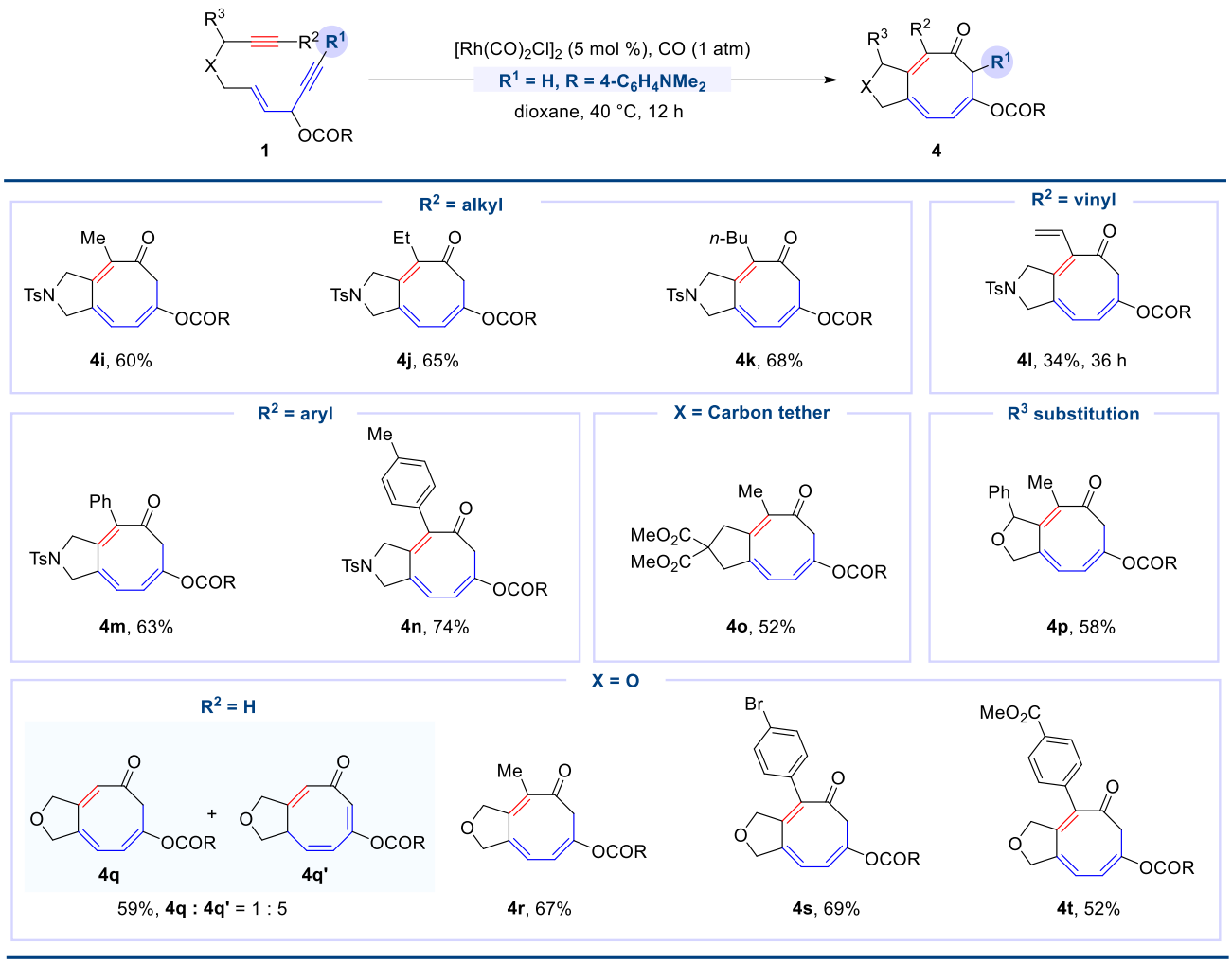

Figure 3. Substrate scope of Rh-catalyzed [5 + 1 + 2] cycloaddition of YACEs and CO. Reaction conditions: **1** (0.1 mmol), $[Rh(CO)_2Cl]_2$ (5 mol %), dioxane (4 mL), 40 °C, CO (1 atm). The yield of every substrate reported here was an average of two runs.

Reaction Mechanism of [5 + 1 + 2] Reaction

We then applied quantum chemical calculations to understand the [5 + 1 + 2] reaction using **1r** as the model substrate. Figure 4 shows the key steps involved in the competing [5 + 1 + 2] and [4 + 2 + 1] pathways. The other steps in the [5 + 1 + 2] pathway and the disfavored [5 + 2 + 1] pathway are given in Figure 5.

Similar to both [5 + 2 + 1] of ene-vinylcyclopropanes and CO[8e] and [4 + 2 + 1] reaction of ene/yne-ene-allenes and CO,[6] the catalytic species was proposed to be a monomeric form (the resting state could be formed by $[Rh(CO)_2Cl_2]_2$, substrate, solvent, but the exact form is unknown now). As shown in Figure 4, formation of **IN1** from the dimer and substrate is endergonic by 8.0 kcal/mol, which is followed by the stepwise 1,2-acyloxy migration. The nucleophilic attack between carbonyl oxygen and alkyne (via **TS1** to give **IN2**), coordination of alkene in the five-carbon synthon to Rh (via **TS2** to **IN3**) and the carbon-oxygen cleavage (via **TS3** to form the 5-membered rhodacycle **IN4**) are three consecutive steps of the stepwise migration process. The activation Gibbs free energy of 1,2-acyloxy migration is 14.1 kcal/mol (from **IN1** to **TS2**).

The followed step in the [5 + 1 + 2] reaction is CO insertion, which starts from coordination of the oxygen tether to Rh in **IN4**, affording **IN5** (Figure 5). Then CO migratory insertion occurs via **TS4** to give 7-membered rhodacycle **IN6**, with an activation free energy of 6.7 kcal/mol. Subsequently, **IN6** can isomerize to form a more stable

intermediate, **IN7**, which then undergoes another isomerization (giving **IN8**) to facilitate the followed alkyne coordination (giving **IN9**) and insertion (via **TS5** to give nine-membered rhodacycle **IN10,** with an activation free energy of 17.3 kcal/mol). After that, reductive elimination of **IN10** (via **TS6**) and catalyst transfer happen easily, producing the [5 + 1 + 2] cycloadduct **4r'**. Finally, **4r'** undergoes intramolecular [1,5]-H shift (this is an off-cycle process) to give a more stable product, **4r**, via the envelope-shape transition state **TS7** (with an activation free energy of 25.2 kcal/mol).

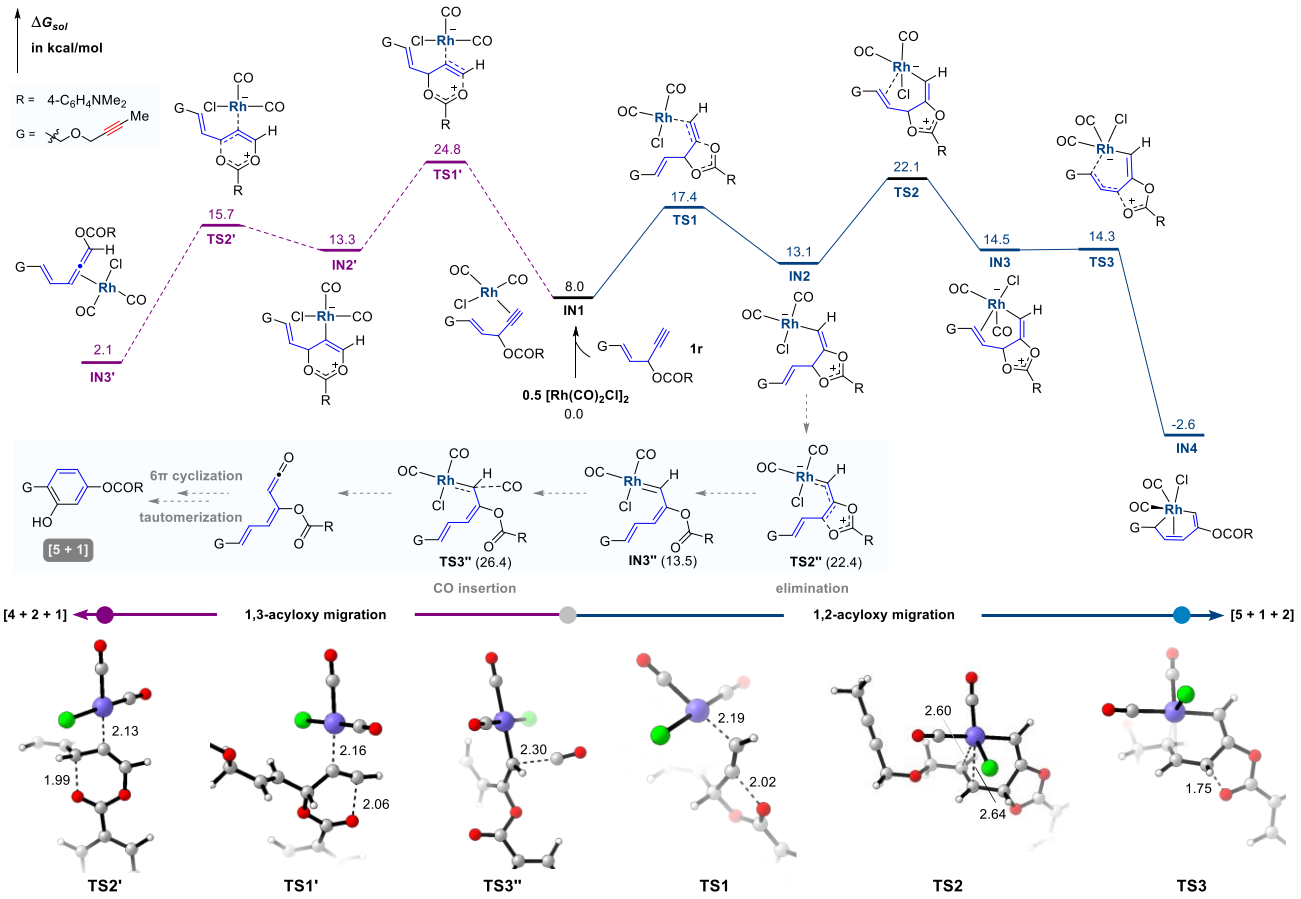

Figure 4. Competition between 1,3-acyloxy migration and 1,2-acyloxy migration for YACE substrate **1r**. Computed at the DLPNO-CCSD(T)/def2-TZVPP:SMD(1,4-dioxane)//SMD(1,4-dioxane)/BMK/def2-SVP level. For each 3D molecular structures, only the reaction center part was shown for clarity. Bond distances are reported in Ångstrom.

We can conclude that in the [5 + 1 + 2] reaction, 1,2-acyloxy migration (alkene coordination) is the rate-determining step in the catalytic cycle (from the resting state to **TS2**). The overall activation Gibbs free energy of the [5 + 1 + 2] reaction is larger than 22.1 kcal/mol: the overall activation free energy is the sum of 22.1 kcal/mol (from monomer of catalyst to **TS2**) and energy required to generate monomer from the unknown resting state. Since the [1,5]-H shift step requires an activation free energy of 25.2 kcal/mol and we proposed that the overall activation free energy of the present [5 + 1 + 2] is at least 25.2 kcal/mol or a little higher. This estimation is reasonable considering the fact that the [5 + 1 + 2] reaction usually finished at 40 °C in about 12 h.

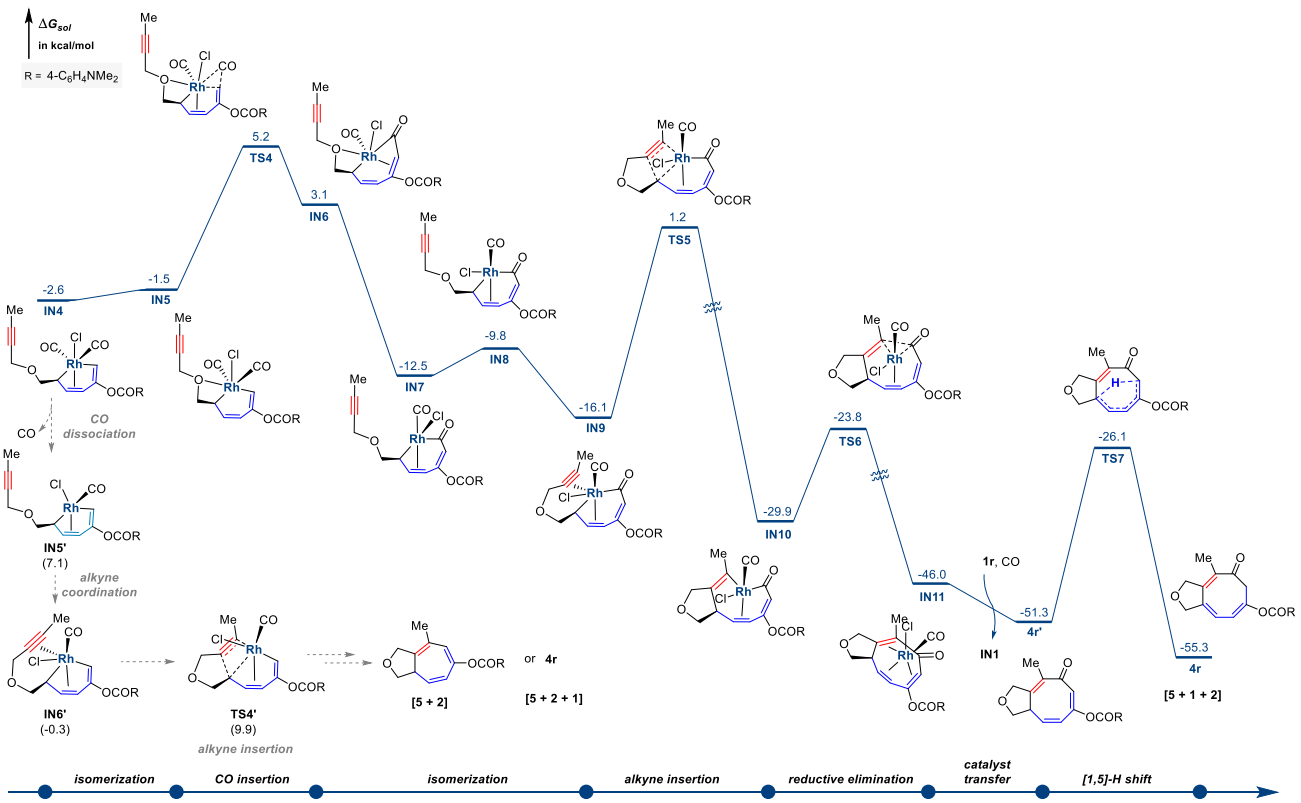

Figure 5. Gibbs energy profile for [5 + 1 + 2] cycloaddition reaction and other competition pathways of model substrate **1r**. Computed at the DLPNO-CCSD(T)/def2-TZVPP:SMD(1,4-dioxane)//SMD(1,4-dioxane)/BMK/def2-SVP level.

Substitution Effects for the Competing 1,2- and 1,3-Acyloxy Migrations

Except for 1,2-acyloxy migration, there is another 1,3-acyloxy migration process for **IN1** leading to [4 + 2 + 1] product (Figure 4). **IN1** firstly undergo nucleophilic addition of ester's carbonyl group via **TS1'** to give **IN2'**, with an activation free energy of 16.8 kcal/mol. Easy reductive C–O cleavage occurs via **TS2'** to give **IN3'**, which could undergo the several followed steps to afford the final [4 + 2 + 1] product. The selectivity between [5 + 1 + 2] and [4 + 2 + 1] pathways is determined by the relative free energy of **TS2** and **TS1'**. Here **TS2** is 2.7 kcal/mol more stable than **TS1'**. Thus, no [4 + 2 + 1] product is observed, agreeing with experiments.

We found that substitutions (R^1) on the terminal position of alkyne moiety of the YACEs have significant impacts on the competition between the 1,3- and 1,2-acyloxy migration processes, which bifurcates to deliver [5 + 1 + 2], [5 + 2] or [4 + 2 + 1] products (Figure 6A). When R^1 = CO_2Et or CF_3 (substrate **1d-e**), experimentally we obtained 1,2-acyloxy migration products ([5 + 2] products, see Figure 2B). Our quantum chemical calculations agreed with the experimental observations and showed that the activation free energy difference $\Delta\Delta G_1^{\ddagger}$ (the value of $\Delta G_2^{\ddagger} - \Delta G_1^{\ddagger}$, see Figure 6A) are 9.8 and 12.5 kcal/mol, favoring 1,2-acyloxy migration. But when R^1 = Ph or Me, 1,3-acyloxy migration products ([4 + 2 + 1] products) are dominant because 1,3-acyloxy migration is 3.0 and 5.2 kcal/mol favored over 1,2-acyloxy migration for Ph and Me, respectively. Experimentally, we obtained [4 + 2 + 1] products for substrate **1a** and **1b** (Figure 2A), consistent with the computational results.

Calculations predicted that for R^1 = H, 1,2-acyloxy migration is still favored over 1,3-acyloxy migration by 0.6 kcal/mol. This is close (although slightly underestimated) to the experimental result qualitatively: both [5 + 1 + 2] and [5 + 1] products via 1,2-acyloxy migration (Figure 2C) were observed. We found that the activation free energy difference $\Delta\Delta G^{\ddagger}$ is highly corelated with Hammett constant[9] σ_p (the R^2 value for the linear regression is 0.98), which

represents the electronic properties of a substituent. Electron-withdrawing group is beneficial to 1,2-acyloxy migration since it can stabilize the Rh anion in the coordination transition states. Similar trend was also found in Au-catalyzed propargylic ester rearrangement.[10]

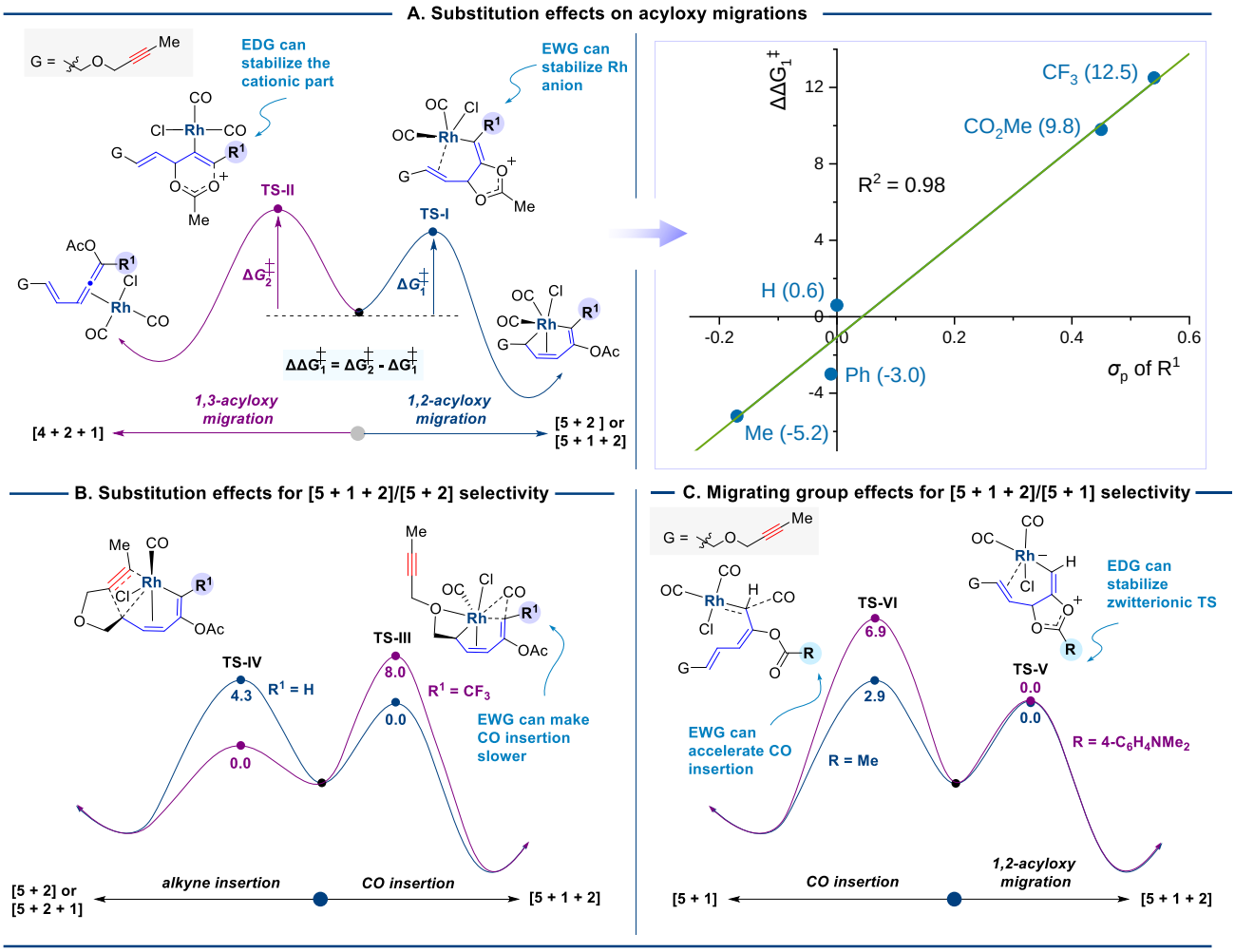

Figure 6. Effects of substitution and migrating group. (A) Substitution effects on acyloxy migrations. (B) Substitution effects on competition between [5 + 2] and [5 + 1 + 2] reaction pathways. (C) Effect of migrating group on competition between [5 + 1 + 2] and [5 + 1] reaction pathways. EDG, electron-donating group; EWG, electron-withdrawing group. Computed at DLPNO-CCSD(T)/def2-TZVPP:SMD(DCE)//SMD(DCE)/BMK/def2-SVP level.

Substitution Effects for the Competing [5 + 1 + 2], [5 + 2 + 1] and [5 + 2] Pathways

Once **IN4** is generated, it has two other possible reaction pathways to compete with the [5 + 1 + 2] pathway (Figure 5). These two pathways are [5 + 2] and [5 + 2 + 1] pathways, both of which involve CO dissociation/alkyne coordination/alkyne insertion (via **TS4'**) steps (see the bottom part of Figure 5). However, they are 4.7 kcal/mol disfavored over [5 + 1 + 2] pathway via **TS4**, because CO is a good migratory insertion component. It should be noted that once alkyne insertion occurs, [5 + 2] pathway is favored over [5 + 2 + 1] pathway due to the fast reductive elimination step in the former (see SI for details).

The competition between [5 + 1 + 2] and [5 + 2] reactions depends on the R^1 group in the alkyne moiety of the substrates, because R^1 have a significant impact on the relative free energy of the CO insertion and alkyne insertion transition states, **TS-III** and **TS-IV**, respectively (Figure 6B). Our calculations indicated that, the [5 + 1 + 2] pathway

via CO insertion is favored over the [5 + 2] pathway when R^1 = H by 4.3 kcal/mol. While the [5 + 2] pathway via alkyne insertion becomes much more favored when a more electron deficient R^1, here is CF_3, is used.

These computational predictions are consistent with the experimental results shown in Figures 2B and 2C. We proposed that the electron-withdrawing group can reduce the nucleophilicity of the adjacent carbon atom of R^1 substituent, consequently slowing down the CO insertion. But this has little impact on the alkyne insertion step since R^1 is far away from the reaction center in this step.

Effects of Migrating Group on the Competition between [5 + 1 + 2] and [5 + 1] Pathways

Finally, we present reasons for generating side [5 + 1] product in some substrates. We proposed a new pathway shown in the bottom of Figure 4. Intermediate **IN2** isomerizes via **TS2"** to generate Rh-carbene complex **IN3"**, with an activation free energy 9.3 kcal/mol. Subsequently, irreversible CO insertion via **TS3"** occurs to give the ketene intermediate,[11] with an activation free energy of 12.9 kcal/mol. The ketene intermediate undergoes 6π cyclization/isomerization to give the final [5 + 1] product, which is very easy (shown in the SI). This mechanism is favored compared to the mechanism in literature,[7b-c] where the ketene is formed via reductive elimination of **IX** (see Figure 1 and SI for details).

Comparison of the [5 + 1 + 2] and [5 + 1] pathways demonstrates that the selectivity is determined by 1,3-acyloxy migration (via **TS2**) and CO insertion of Rh carbene (via **TS3"**). Thus, [5 + 1] is not feasible since **TS2** is 4.3 kcal/mol favored over **TS3"**, consistent with the experiment that no [5 + 1] product for **1r** and other substrates with electron donating 4-$C_6H_4NMe_2$ (R group) as substrate.

Various migrating groups exert distinct influences on the selectivity between [5 + 1 + 2] and [5 + 1] pathways (Figure 6). In experimental tests, substrate **1r** with R = 4-$C_6H_4NMe_2$ exclusively yielded the [5 + 1 + 2] product **4r**, whereas substrates **1f** and **1h**, with an acyloxy group (R = Me), produced both [5 + 1 + 2] and [5 + 1] products (see Figure 2C). To comprehend these differences, we computationally examined the 1,2-acyloxy migration (**TS-V**) and CO insertion of the Rh carbene (**TS-VI**). For R = 4-$C_6H_4NMe_2$, **TS-VI** is 6.9 kcal/mol disfavored over **TS-V**, consistent with experiments. As for R = Me, **TS-V** exhibited a smaller preference (2.9 kcal/mol) over **TS-VI**, suggesting almost no [5 + 1] product could be generated. Experimentally, both [5 + 1 + 2] (dominant) and [5 + 1] products were formed (see Figure 2C). Here we proposed that these is some overestimation of the [5 + 1 + 2] pathway in the calculations. But the trend here is obvious that electron-donating group favors [5 + 1 + 2] reaction. Why?

We attribute the above selectivity to the R group's ability to tune the electrophilicity of the Rh carbene, influencing CO insertion into the Rh-carbene. Stronger electron withdrawal ability of the R group enhances electrophilicity of Rh-carbene, facilitating CO insertion. Additionally, 1,2-acyloxy migration is promoted when the R group is more electron-donating, stabilizing the cationic moiety of **TS-V**. In essence, selecting an R group with higher electron-donating ability can enhance [5 + 1 + 2] reaction with respect to [5 + 1] cycloaddition.

CONCLUSIONS

In summary, we experimentally observed that, under the Rh catalysis, the reaction of yne-3-acyloxy-1,4-enynes (YACEs) and CO delivers different products, [5 + 1], [5 + 2], [4 + 2 + 1] and [5 + 1 + 2] cycloadducts, depending on the used substituents in the substrates (Figure 1). By choosing terminal alkyne as the 2π component and the critical migrating group with R=4-$C_6H_4NMe_2$ in the migrating group, the first [5 + 1 + 2] reaction has been achieved. This reaction has broad scope and can be utilized to synthesize highly functionalized eight-membered carbocycles. Quantum chemical calculations have been applied to understand why this reaction prefers [5 + 1 + 2] reaction (CO insertion ahead of alkyne insertion) instead of [5 + 2 + 1] reaction (alkyne insertion ahead of CO insertion). In addition, the generation of the side product via [5 + 1] reaction has been analyzed and the mechanism for this reaction was investigated, showing CO insertion to form ketenes from Rh-carbene is favored when using R=CH_3 in the migrating

acetoxy group in YACEs. By choosing other substituent in the alkyne moiety of the YACEs, [4 + 2 + 1] and [5 + 2] reaction can be realized. The present [5 + 1 + 2] reaction will serve as a new way to synthesize challenging eight-membered carbocycle. This represents also a new advance for carbonylative cyclization reactions using 3-acyloxy-1,4-enynes as a five-carbon synthon.[2e]

COMPUTATIONAL METHODS

All the density functional theory (DFT) calculations were carried out by using Gaussian 09E.01 software.[12] Pruned integrationgrids with 99 radial shells and 590 angular points per shell were used in DFT calculations. Geomertry optimizations were performed using BMK[13] functional together with def2-SVP[14] as basis set and SMD[15] (in dioxane or DCE) as the sovation model unless otherwise specified. Unscaled harmonic frequency calculations were performed at the same level to validate each structure as either a minimum or a transition state and to evaluate its zero-point energy and thermal corrections at 298.15 K. Solvation effects were also calculated at the same level. For each optimized structures, single-point energy refinement was comupted at DLPNO-CCSD(T)[16]/def2-TZVPP[14] level (with def2-TZVPP/C[17] auxiliary basis set) using ORCA 4.2.1 software package.[18] During the single-point energy calculations, the seetings of "TightPNO" and "TightSCF" were also applied unless otherwise specified. 3D moelcular structures were generated by CYLView.[19] The standard state for CO is 5.1 mM (in dioxane)[20] and 5.5 mM (in DCE)[6,21] and the other species have standard states of 1.0 M.

AUTHOR INFORMATION

Corresponding Author

*Zhi-Xiang Yu, orcid.org/0000-0003-0939-9727; Email: yuzx@pku.edu.cn.

Author Contributions

†Q.C., P.Z., and B.-W. L. contributed equally to this work.

Conflict of Interest

The authors declare no conflict of interest.

ACKNOWLEDGMENT

This work was supported by the National Natural Science Foundation of China (21933003) and High-Performance Computing Platform of Peking University. We thank Mr. Chenkai Fan of Peking University for helping with some experiments. Dr. Jie Su in Peking University was thanked for X-ray single crystal analysis.

REFERENCES

1. (a) Molander, G. A. Diverse Methods for Medium Ring Synthesis. *Acc. Chem. Res.* **1998**, *31*, 603−609. (b) Yet, L. Metal-Mediated Synthesis of Medium-Sized Rings. *Chem. Rev.* **2000**, *100*, 2963−3008. (c) Battiste, M. A.; Pelphrey, P. M.; Wright, D. L. The Cycloaddition Strategy for the Synthesis of Natural Products Containing Carbocyclic Seven-Membered Rings. *Chem. Eur. J.* **2006**, *12*, 3438–3447. (d) de Oliveira, K. T.; Servilha, B. M.; de C. Alves, L.; Desiderá, A. L.; Brocksom, T. J. The Synthesis of Seven Membered Rings in Natural Products. In *Studies in Natural Products Chemistry,* Atta ur, R., Ed. Elsevier: 2014; Vol. 42, pp 421−463.
2. (a) Yu, Z.-X.; Wang, Y.; Wang, Y. Transition-Metal-Catalyzed Cycloadditions for the Synthesis of Eight-Membered Carbocycles. *Chem. Asian J.* **2010**, *5*, 1072–1088. (b) Trost, B. M.; Zuo, Z.; Schultz, J. E. Transition-Metal Catalyzed Cycloaddition Reactions to Access Seven-Membered Rings. *Chem. Eur. J.* **2020**, *26*, 15354–15377. (c) Hu, Y.-J.; Li, L.-X.; Han, J.-C.; Min, L.; Li, C.-C. Recent Advances in the Total Synthesis of Natural

Products Containing Eight-Membered Carbocycles (2009–2019). *Chem. Rev.* **2020**, *120*, 5910–5953. (d) Wang, L.-N.; Yu, Z.-X. Transition-Metal-Catalyzed Cycloadditions for the Synthesis of Eight-Membered Carbocycles: An Update from 2010 to 2020. *Chin. J. Org. Chem*., **2020**, *40*, 3536–3558. (e) Li, C.-L.; Yu, Z.-X. Progress in Transition-Metal-Catalyzed Carbonylative Cycloadditions Using Carbon Monoxide. *Chin. J. Org. Chem.* **2023**, *43*, DOI: 10.6023/cjoc202310003.

3. (a) Blaszczyk, S. A.; Glazier, D. A.; Tang, W. Rhodium-Catalyzed (5 + 2) and (5 + 1) Cycloadditions Using 1,4-Enynes as Five-Carbon Building Blocks. *Acc. Chem. Res.* **2020**, *53*, 231−243. (b) Shu, X.; Huang, S.; Shu, D.; Guzei, I. A.; Tang, W. Interception of a Rautenstrauch Intermediate by Alkynes for [5+2] Cycloaddition: Rhodium-Catalyzed Cycloisomerization of 3-Acyloxy-4-Ene-1,9-Diynes to Bicyclo[5.3.0]Decatrienes. *Angew. Chem., Int. Ed.* **2011**, *50*, 8153–8156. (c) Shu, X.-Z.; Li, X.; Shu, D.; Huang, S.; Schienebeck, C. M.; Zhou, X.; Robichaux, P. J.; Tang, W. Rhodium-Catalyzed Intra- and Intermolecular [5 + 2] Cycloaddition of 3-Acyloxy-1,4-Enyne and Alkyne with Concomitant 1,2-Acyloxy Migration. *J. Am. Chem. Soc.* **2012**, *134*, 5211–5221. (d) Shu, X.; Schienebeck, C. M.; Song, W.; Guzei, I. A.; Tang, W. Transfer of Chirality in the Rhodium-Catalyzed Intramolecular [5+2] Cycloaddition of 3-Acyloxy-1,4-Enynes (ACEs) and Alkynes: Synthesis of Enantioenriched Bicyclo[5.3.0]Decatrienes. *Angew. Chem., Int. Ed.* **2013**, *52*, 13601–13605. (e) Schienebeck, C. M.; Robichaux, P. J.; Li, X.; Chen, L.; Tang, W. Effect of Ester on Rhodium-Catalyzed Intermolecular [5+2] Cycloaddition of 3-Acyloxy-1,4-Enynes and Alkynes. *Chem. Commun.* **2013**, *49*, 2616–2618. (f) Schienebeck, C. M.; Li, X.; Shu, X.; Tang, W. 3-Acyloxy-1,4-Enyne: A New Five-Carbon Synthon for Rhodium-Catalyzed [5 + 2] Cycloadditions. *Pure and Applied Chemistry* **2014**, *86*, 409–417. (g) Schienebeck, C. M.; Song, W.; Smits, A. M.; Tang, W. Rhodium-Catalyzed Intermolecular [5+1] and [5+2] Cycloadditions Using 1,4-Enynes with an Electron-Donating Ester on the 3-Position. *Synthesis* **2015**, *47*, 1076–1084. (h) Shu, X.; Schienebeck, C. M.; Li, X.; Zhou, X.; Song, W.; Chen, L.; Guzei, I. A.; Tang, W. Rhodium-Catalyzed Stereoselective Intramolecular [5 + 2] Cycloaddition of 3-Acyloxy 1,4-Enyne and Alkene. *Org. Lett.* **2015**, *17*, 5128–5131. (i) Li, X.; Song, W.; Ke, X.; Xu, X.; Liu, P.; Houk, K. N.; Zhao, X.; Tang, W. Rhodium-Catalyzed Intramolecular [5+2] Cycloaddition of Inverted 3-Acyloxy-1,4-Enyne and Alkyne: Experimental and Theoretical Studies. *Chem. – Eur. J.* **2016**, *22*, 7079–7083. (j) Song, W.; Lynch, J. C.; Shu, X.; Tang, W. Rhodium-Catalyzed [5+2] Cycloaddition of 3-Acyloxy-1,4-Enyne with Alkene or Allene. *Adv. Synth. Catal.* **2016**, *358*, 2007–2011.
4. Tian, Z.; Cui, Q.; Liu, C.; Yu, Z. Rhodium-Catalyzed [4+2+1] Cycloaddition of In Situ Generated Ene/Yne-Ene-Allenes and CO. *Angew. Chem., Int. Ed.* **2018**, *57*, 15544–15548.
5. Xu, X.; Liu, P.; Shu, X.; Tang, W.; Houk, K. N. Rh-Catalyzed (5+2) Cycloadditions of 3-Acyloxy-1,4-Enynes and Alkynes: Computational Study of Mechanism, Reactivity, and Regioselectivity. *J. Am. Chem. Soc.* **2013**, *135*, 9271–9274.
6. Yang, Y.; Tian, Z.-Y.; Li, C.-L.; Yu, Z.-X. Why [4 + 2 + 1] but Not [2 + 2 + 1]? Why Allenes? A Mechanistic Study of the Rhodium-Catalyzed [4 + 2 + 1] Cycloaddition of *In Situ* Generated Ene–Ene–Allenes and Carbon Monoxide. *J. Org. Chem.* **2022**, *87*, 10576–10591.
7. (a) Shu, D.; Li, X.; Zhang, M.; Robichaux, P. J.; Tang, W. Synthesis of Highly Functionalized Cyclohexenone Rings: Rhodium-Catalyzed 1,3-Acyloxy Migration and Subsequent [5+1] Cycloaddition. *Angew. Chem., Int. Ed.* **2011**, *50*, 1346–1349. (b) Ke, X.-N.; Schienebeck, C. M.; Zhou, C.-C.; Xu, X.-F.; Tang, W.-P. Mechanism and Reactivity of Rhodium-Catalyzed Intermolecular [5 + 1] Cycloaddition of 3-Acyloxy-1,4-enyne (ACE) and CO: a Computational Study. *Chin. Chem. Lett.* **2015**, *26*, 730–734. (c) Coskun, D.; Tüzün, N. A DFT study on the mechanism of Rh-catalyzed competitive 1,2- versus 1,3-acyloxy migration followed by [5+1] and [4+1] cycloadditions of 1,4-enynes with CO. *J. Organometallic Chem.* **2017**, *851*, 97–103.
8. For previous example of [5 + 2 + 1] cycloadditions, see: (a) Wender, P. A.; Gamber, G. G.; Hubbard, R. D.; Zhang, L. Three-Component Cycloadditions: The First Transition Metal-Catalyzed [5+2+1] Cycloaddition

Reactions. *J. Am. Chem. Soc.* **2002**, *124*, 2876–2877. (b) Wang, Y.; Wang, J.; Su, J.; Huang, F.; Jiao, L.; Liang, Y.; Yang, D.; Zhang, S.; Wender, P. A.; Yu, Z.-X. A Computationally Designed Rh(I)-Catalyzed Two-Component [5+2+1] Cycloaddition of Ene-Vinylcyclopropanes and CO for the Synthesis of Cyclooctenones. *J. Am. Chem. Soc.* **2007**, *129*, 10060–10061. (c) Huang, F.; Yao, Z.-K.; Wang, Y.; Wang, Y.; Zhang, J.; Yu, Z.-X. Rh^{I}-Catalyzed Two-Component [(5+2)+1] Cycloaddition Approach toward [5-8-5] Ring Systems. *Chem. Asian J.* **2010**, *5*, 1555–1559. (d) Wang, L.-N.; Huang, Z.; Yu, Z. X. Synthesis of Polycyclic n/5/8 and n/5/5/5 Skeletons Using Rhodium-Catalyzed [5 + 2 + 1] Cycloaddition of Exocyclic-ene-vinylcyclopropanes and Carbon Monoxide. *Org. Lett.* **2023**, *25*, 1732–1736. (e) Wang, Y.; Liao, W.; Wang, Y.; Jiao, L.; Yu, Z.-X. Mechanism and Stereochemistry of Rhodium-Catalyzed [5 + 2 + 1] Cycloaddition of Ene−Vinylcyclopropanes and Carbon Monoxide Revealed by Visual Kinetic Analysis and Quantum Chemical Calculations. *J. Am. Chem. Soc.* **2022**, *144*, 2624–2636.

9. (a) Hansch, C.; Leo, A.; Taft, R. W. A survey of Hammett substituent constants and resonance and field parameters. *Chem. Rev.* **1991**, *91*, 165–195. For application of Hammett constant in other nonaromatic systems, see: (b) Charton, M.; Meislich, H. *J. Am. Chem. Soc.* **1958**, *80*, 5940–5943. (c) Jabłoński, M; Krygowski, T. M. On differences in substituent effects in substituted ethene and acetylene derivatives and their boranyl analogs. *Structural Chemistry* **2021**, *32*, 285–296.
10. Jiang, J.; Liu, Y.; Hou, C.; Li, Y.; Luan, Z.; Zhao, C.; Ke, Z. Rationalization of the selectivity between 1,3- and 1,2-migration: a DFT study on gold(i)-catalyzed propargylic ester rearrangement. *Org. Biomol. Chem.* **2016**, *14*, 3558−3563.
11. Dai, P.; Ogunlana, A. A.; Bao, X. Mechanistic Insights into Cyclopropenes-Involved Carbonylative Carbocyclization Catalyzed by Rh(I) Catalyst: A DFT Study. *J. Org. Chem.* **2018**, *83*, 12734−12743.
12. Frisch, M. J.; Trucks, G. W.; Schlegel, H. B.; Scuseria, G. E.; Robb, M. A.; Cheeseman, J. R.; Scalmani, G.; Barone, V.; Mennucci, B.; Petersson, G. A.; Nakatsuji, H.; Caricato, M.; Li, X.; Hratchian, H. P.; Izmaylov, A. F.; Bloino, J.; Zheng, G.; Sonnenberg, J. L.; Hada, M.; Ehara, M.; Toyota, K.; Fukuda, R.; Hasegawa, J.; Ishida, M.; Nakajima, T.; Honda, Y.; Kitao, O.; Nakai, H.; Vreven, T.; Montgomery, J. A., Jr.; Peralta, J. E.; Ogliaro, F.; Bearpark, M.; Heyd, J. J.; Brothers, E.; Kudin, K. N.; Staroverov, V. N.; Keith, T.; Kobayashi, R.; Normand, J.; Raghavachari, K.; Rendell, A.; Burant, J. C.; Iyengar, S. S.; Tomasi, J.; Cossi, M.; Rega, N.; Millam, J. M.; Klene, M.; Knox, J. E.; Cross, J. B.; Bakken, V.; Adamo, C.; Jaramillo, J.; Gomperts, R.; Stratmann, R. E.; Yazyev, O.; Austin, A. J.; Cammi, R.; Pomelli, C.; Ochterski, J. W.; Martin, R. L.; Morokuma, K.; Zakrzewski, V. G.; Voth, G. A.; Salvador, P.; Dannenberg, J. J.; Dapprich, S.; Daniels, A. D.; Farkas, Ö.; Foresman, J. B.; Ortiz, J. V.; Cioslowski, J.; Fox, D. J. *Gaussian 09*, Revision E.01; Gaussian, Inc.: Wallingford, CT, 2013.
13. Boese, A. D.; Martin, J. M. L. Development of Density Functionals for Thermochemical Kinetics. *J. Chem. Phys.* **2004**, *121*, 3405−3416.
14. (a) Weigend, F.; Ahlrichs, R. Balanced basis sets of split valence, triple zeta valence and quadruple zeta valence quality for H to Rn: Design and assessment of accuracy. *Phys. Chem. Chem. Phys.* **2005**, *7*, 3297−3305. (b) Andrae, D.; Häußermann, U.; Dolg, M.; Stoll, H.; Preuß, H. Energy-Adjusted Ab Initio Pseudopotentials for the Second and Third Row Transition Elements. *Theor. Chim. Acta* **1990**, *77*, 123−141.
15. Marenich, A. V.; Cramer, C. J.; Truhlar, D. G. Universal Solvation Model Based on Solute Electron Density and on a Continuum Model of the Solvent Defined by the Bulk Dielectric Constant and Atomic Surface Tensions. *J. Phys. Chem. B* **2009**, *113*, 6378−6396.
16. (a) Riplinger, C.; Neese, F. An Efficient and Near Linear Scaling Pair Natural Orbital Based Local Coupled Cluster Method. *J. Chem. Phys.* **2013**, *138*, 034106. (b) Riplinger, C.; Sandhoefer, B.; Hansen, A.; Neese, F. Natural Triple Excitations in Local Coupled Cluster Calculations with Pair Natural Orbitals. *J. Chem. Phys.* **2013**, *139*, 134101. (c) Neese, F.; Atanasov, M.; Bistoni, G.; Maganas, D.; Ye, S. Chemistry and Quantum Mechanics in 2019: Give Us Insight *and* Numbers. *J. Am. Chem. Soc.* **2019**, *141*, 2814−2824.

17. Hellweg, A.; Hättig, C.; Höfener, S. Klopper, W. Optimized accurate auxiliary basis sets for RI-MP2 and RI-CC2 calculations for the atoms Rb to Rn. *Theor. Chem. Acc.* **2007**, *117*, 587−597.
18. (a) Neese, F. The ORCA Program System. *Wiley Interdiscip. Rev.: Comput. Mol. Sci.* **2012**, *2*, 73−78. (b) Neese, F. Software Update: The ORCA Program System, Version 4.0. *Wiley Interdiscip. Rev.: Comput. Mol. Sci.* **2017**, *8*, e1327.
19. Legault, C. Y. CYLview20; Université de Sherbrooke, 2020; http://www.cylview.org (accessed 24 January, 2021).
20. Veleckis, E.; Hacker, D. S. Solubility of Carbon Monoxide in 1,4-Dioxane. *J. Chem. Eng. Data* **1984**, *29*, 36−39.
21. Skirrow, F. W. Über die Löslichkeit von Kohlenoxyd in binären organischen Gemischen. Z. *Phys. Chem.* **1902**, *41U*, 139.